Volume 58
Number 53
7 July 2022
Pages 7327–7440

ChemComm

Chemical Communications

rsc.li/chemcomm

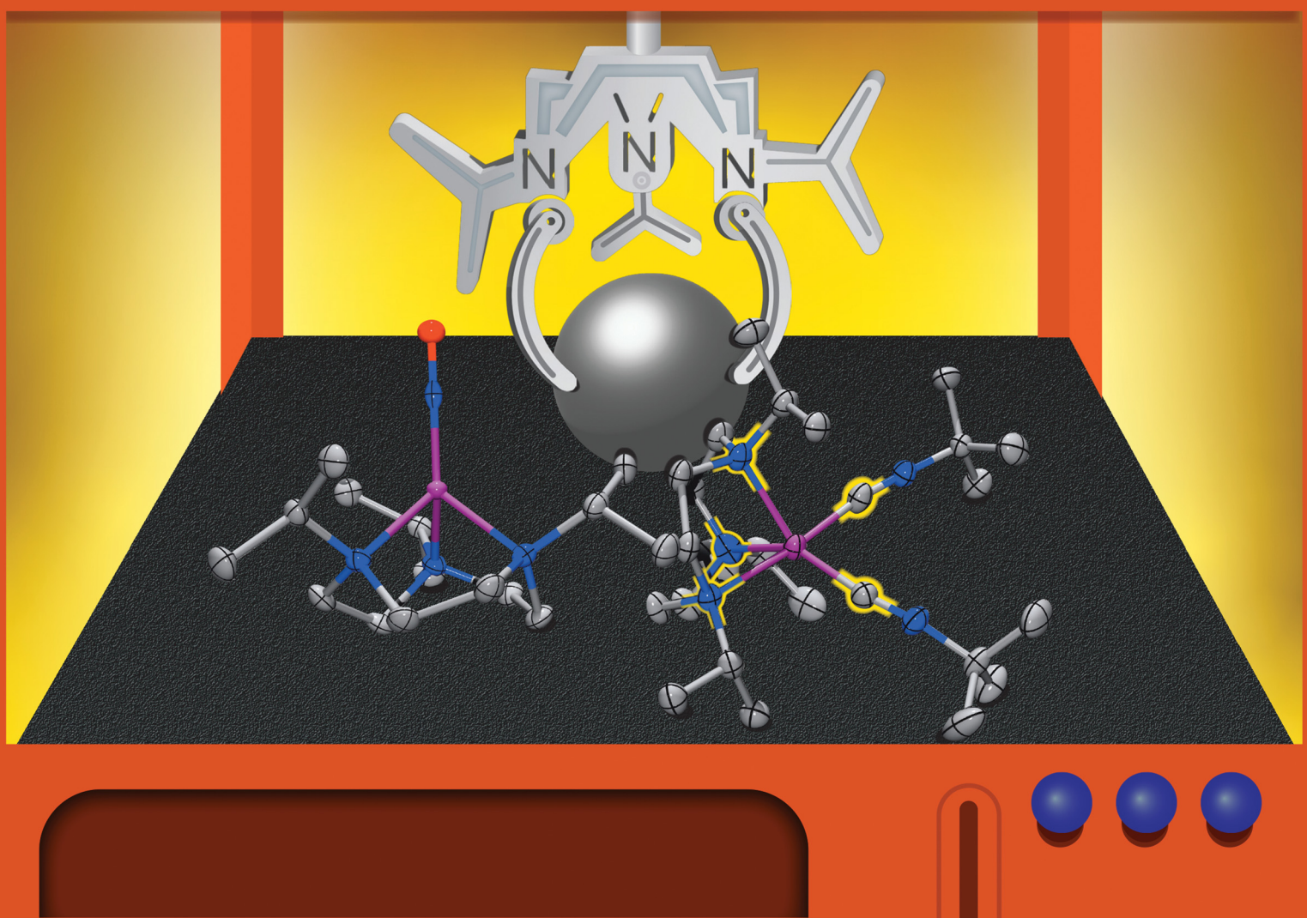

ISSN 1359-7345

ROYAL SOCIETY OF CHEMISTRY

COMMUNICATION

Liviu M. Mirica *et al.*

A five-coordinate Ni(I) complex supported by 1,4,7-triisopropyl-1,4,7-triazacyclononane

ChemComm

COMMUNICATION

View Article Online
View Journal | View Issue

Cite this: *Chem. Commun.*, 2022, **58**, 7360

Received 4th May 2022,
Accepted 9th June 2022

DOI: 10.1039/d2cc02516g

rsc.li/chemcomm

A five-coordinate Ni(I) complex supported by 1,4,7-triisopropyl-1,4,7-triazacyclononane†

Leonel Griego, Toby J. Woods and Liviu M. Mirica *

An isolated Ni(II)-nitrosyl complex supported by the bulky tridentate 1,4,7-triisopropyl-1,4,7-triazacyclononane (iPr_3TACN) ligand was obtained from the reaction of a Ni(II) dimethyl complex with $NOPF_6$, suggesting the *in situ* formation of a Ni(I) species that reacts with the resulting NO product. Use of a π-acceptor ancillary isocyanide ligand led to the isolation and characterization of an uncommon 5-coordinate Ni(I) complex supported by the iPr_3TACN ligand and *tert*-butylisocyanide.

Ni complexes are known to be efficient catalysts for various types of cross-coupling reactions. Although many Ni(0)/Ni(II) species have been reported as intermediates Ni-mediated catalysis, newer studies suggest that their odd-electron Ni(I)/Ni(III) counterparts are also viable catalytic intermediates.[1–4] More recent studies have focused on accessing and isolating rare Ni(III) organometallic complexes; nevertheless, the related organometallic Ni(I) species are sometimes overlooked.[2]

Several Ni(I) coordination complexes have been reported,[5] and such species are essential in the catalytic process as they can undergo radical or oxidative addition of various electrophiles, key steps in a catalytic cycle.[6–10] For example, there are only a few examples involving an oxidative addition of an alkyl or aryl halide to a Ni(I) metal center.[11–16] While the latter complexes were also supported by N-based ligands, none of them employed a macrocyclic ligand. Our group has previously reported the isolation of Ni complexes in the +2, +3, and +4 oxidation states stabilized by various N-based macrocyclic ligands. In these systems a Ni(I) intermediate is commonly proposed to form *in situ* upon the reductive elimination of C–C bond formation products, yet due to the hard-donating nature of the employed ligands we have never observed or isolated a Ni(I) complex.[17–25] In our efforts to isolate low-valent Ni(I) complexes we have employed the soft-donor macrocyclic ligand *P*,*P*′-ditertbutyl-2,11-diphosphonito[3.3](2,6)pyridinophane (N2P2) in combination with isocyanides,[26] yet the use of N-donor macrocycles to stabilize Ni(III) species has remained elusive. More recently, we have employed the bulky tridentate N-donor ligand 1,4,7-triisopropyl-1,4,7-triazacyclononane (iPr_3TACN) to explore the oxidatively induced reactivity of the (iPr_3TACN)Ni(II)Me_2 (**1**) complex. Herein, we report the use of iPr_3TACN and an π-acceptor ancillary isocyanide ligand that leads to the isolation and characterization of an uncommon 5-coordinate Ni(I) complex supported by the iPr_3TACN ligand and *tert*-butylisocyanide.

Interestingly, during the oxidatively induced reactivity studies of **1**, the use of 0.9 equiv. $NOPF_6$ leads to the formation of [(iPr_3TACN)Ni(II)NO]PF_6 (**2**) as a violet powder in 73% yield (Fig. 1).[27] X-Ray quality crystals were obtained and the solid-state structure was determined to reveal a four-coordinate Ni(II) tetrahedral complex with a geometry index of τ_4 = 0.74. Examining the Ni–N bond distances, three equivalent Ni–N bonds

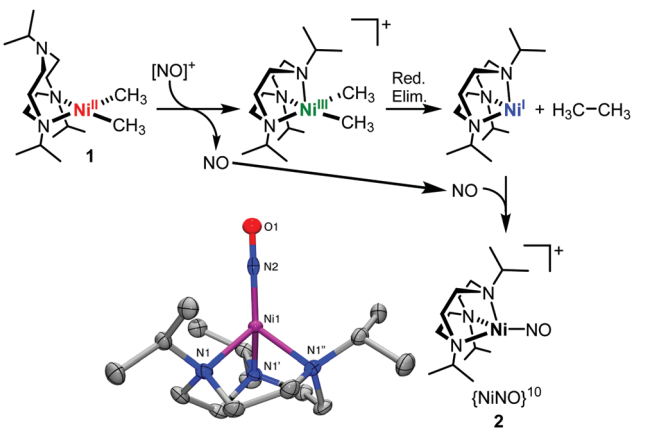

Fig. 1 Synthetic scheme and mechanism for the formation of **2** and the ORTEP representation of its solid-state structure with 50% probability ellipsoids. Hydrogen atoms and anions omitted for clarity. Selected bond lengths (Å): Ni1–N1, 2.042(2); Ni1–N2, 1.677(4) N2–O1, 1.123(5). Selected bond angle (°): Ni1–N4–O1, 180.0.

Department of Chemistry University of Illinois at Urbana Champaign 600 S. Mathews Avenue, Urbana, Illinois, 61801, USA. E-mail: mirica@illinois.edu

† Electronic supplementary information (ESI) available. CCDC 2167418 (**2**), 2166722 (**3**), 2166723 (**4**), 2166724 (**5**), and 2167752 ([(iPr_3TACN)Ni(II)($NOCH_3NO$)]PF_6). For ESI and crystallographic data in CIF or other electronic format see DOI: https://doi.org/10.1039/d2cc02516g

with a length of 2.042 Å were observed. In addition, the Ni–N_{NO} bond distance of 1.646 Å and the N–O bond length of 1.12 Å are slightly shorter than other Ni(II)–NO complexes reported in the literature,[28–31] but consistent with a N≡O triple bond character that is further confirmed by the linear Ni–N≡O interaction with a Ni1–N4–O1 bond angle of 180°. The IR spectrum of **2** reveals a distinctive N≡O bond stretch at 1770 cm^{-1}, which is well within the range for a M–N≡O triple bond.[28,29,32] Previous studies with tridentate N-based ligands such as the sterically hindered Tp (hydrotris(pyrazolyl)borate) ligand have proven successful in the isolation and characterization of tetrahedral metal-nitrosyl complexes.[33,34] However, to the best of our knowledge, there are no examples of nitrosyl complexes supported by redox innocent N-based tridentate ligands.[31] Furthermore, the ^{1}H NMR of a solution of **2** reveals a diamagnetic spectrum, which supports the presence of a $\{NiNO\}^{10}$ species based on the classification of Enemark and Feltham,[32] and thus **2** can be viewed as a Ni(0)–NO species if the nitrosyl ligand is treated as NO^+, or a Ni(II)–NO species if the nitrosyl ligand is treated as NO^- (Fig. 1).[35]

Based on the observed reactivity of **1** with $NOPF_6$ and the formation of **2** in high yield, we propose the following mechanism: one-electron oxidation of **1** by $NOPF_6$ followed by rapid reductive elimination of ethane from the transient Ni(III)Me_2 intermediate would generate a Ni(I) species (Fig. 1). Although such a Ni(I) was not observed by Electron Paramagnetic Resonance (EPR) even when the reaction was performed at low temperature, such a species should rapidly react with the NO by-product, formed from the reduction of NO^+, to generate **2** (Fig. 1). Similarly, Warren *et al.* have previously reported the synthesis of a reactive β-diketiminato Ni(I) complex that reacts directly with NO to generate a $\{NiNO\}^{10}$ complex.[29] Interestingly, the reaction of **1** with 1–1.1 equiv. of $NOPF_6$ led to the formation of a mixture of **2** and the blue complex **[(iPr$_3$TACN)Ni(II)(NOCH$_3$NO)]PF$_6$**. The latter *N*-methyl-*N*-nitrosohydroxylaminato complex could not be obtained purely for full characterization, yet characterization by single-crystal X-ray diffraction confirms its identity (Fig. S16, ESI†). These results are consistent with the report of Warren *et al.* in which an *N*-ethyl-*N*-nitrosohydroxylaminato complex was observed in addition to the Ni-nitrosyl complex, and for which a mechanism involving a reaction between a Ni(I) complex and NO was also proposed,[29] and thus providing further support for our proposed mechanism to yield **2** (Fig. 1). Overall, the ability of the iPr$_3$TACN ligand to stabilize a "Ni(0)–NO^+" species, as well as a potential Ni(I) intermediate, prompted us to further pursue the isolation of a (iPr$_3$TACN)Ni(I) complex by employing ancillary π-acceptor ligands that are commonly used to stabilize low-valent metal centers, such as *tert*-butyl isocyanide (^{t}BuNC).[5]

We first synthesized the bis-solvento Ni(II) complex [(iPr$_3$TACN)Ni^{II}(MeCN)$_2$](PF$_6$)$_2$ (**3**) *via* halogen abstraction from a previously reported (iPr$_3$TACN)Ni^{II}Cl$_2$ complex.[36,37] Addition of 2.1 equiv. of TlPF$_6$ to (iPr$_3$TACN)Ni^{II}Cl$_2$ in MeCN yielded a blue solution from which **3** was obtained in 94% yield as a blue crystalline solid. The solid-state structure of complex **3** reveals a 5-coordinate Ni(II) center with a pseudo-square pyramidal geometry and a geometry index of τ_5 = 0.46 (Fig. 3a). The 5-coordinate geometry is supported by three N-donors from the iPr$_3$TACN ligand and coordination of two MeCN molecules, with Ni–N_{ave} bond distances of 2.072 Å for the iPr$_3$TACN ligand and 2.051 Å for the nitrile ligands, respectively. In contrast, the methyl TACN (Me$_3$TACN) analogue adopts an octahedral geometry allowing a third MeCN ligand to coordinate to the metal center to give complex ([(Me$_3$TACN)Ni^{II}(MeCN)$_3$](BF$_4$)$_2$),[38] and thus highlighting the increased steric bulk of the iPr$_3$TACN ligand.

We then prepared [(iPr$_3$TACN)Ni(II)(CN^{t}Bu)$_3$](PF$_6$)$_2$ (**4**) upon the addition of 3.1 equiv. of ^{t}BuNC to a suspension of complex **3** in THF, to yield a pale green solid product in 94% yield (Fig. 2). X-Ray quality crystals of **3** were obtained from vapor diffusion of Et_2O into a MeCN solution, and the solid-state structure reveals an octahedral Ni(II) center with the iPr$_3$TACN ligand coordinating in a κ^3 fashion with an average Ni–N bond length of 2.125 Å (Fig. 3b). To our surprise, the sterically encumbered complex had three ^{t}BuNC molecules coordinated to the metal center, with an average Ni–CNR distance of 1.946 Å and a C≡N bond length of 1.112 Å, which is consistent with previously reported mononuclear Ni(II)–CNR bond distances of similar complexes deposited in the Cambridge Crystal Database (CCDC).[39] Cyclic voltammetry (CV) studies reveal a chemically accessible redox couple at $E_{1/2}$ = −0.92 V *vs.* Fc^+/Fc, with was assigned to Ni^{II}/Ni^{I} redox process (Fig. 4).

Addition of cobaltocene to a suspension of **4** in THF yielded the thermally stable [(iPr$_3$TACN)Ni(I)(CN^{t}Bu)$_2$](PF$_6$) (**5**) in 79% yield. X-Ray quality crystals with a dichroic yellow/green color were obtained from the vapor diffusion of Et_2O into a concentrated MeCN solution. Excitingly, the solid-state structure revealed an unusual 5-coordinate Ni(I) complex adopting a distorted trigonal bipyramidal/square pyramidal structure with a geometry index of τ_5 = 0.53 (Fig. 5). Similar to its Ni(II) analogue, iPr$_3$TACN ligand coordinated in a κ^3 fashion to the Ni center in **5**, yet a slight elongation was observed for with an average Ni–N bond length of 2.199 Å. Furthermore, although we expected a low-coordinate Ni(I) center, we were surprised that two ^{t}BuNC molecules coordinate to the metal center with an average Ni–CNR distance of 1.894 Å, which is consistent with previously reported Ni(I)–CNR bond distances.[40–42] However, we note that the reported Ni(I)–CNR complexes are limited to those containing soft-atom donor ligands, or dinuclear complexes with bridging isocyanides. The C≡N bond lengths in **5** are of interest since we observe an elongation to 1.166 Å compared to its Ni(II) analogue **4**. In addition, Ni(I) complexes tend to prefer low-coordination environments due to their electron rich nature. In fact, there are only a handful of

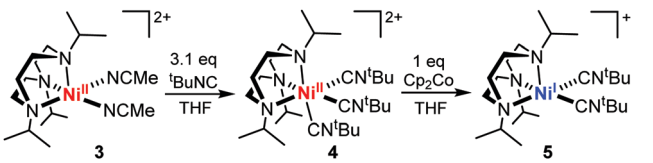

Fig. 2 Synthetic scheme for [(iPr$_3$TACN)Ni(I)(CNtBu)$_2$]PF$_6$ (**5**).

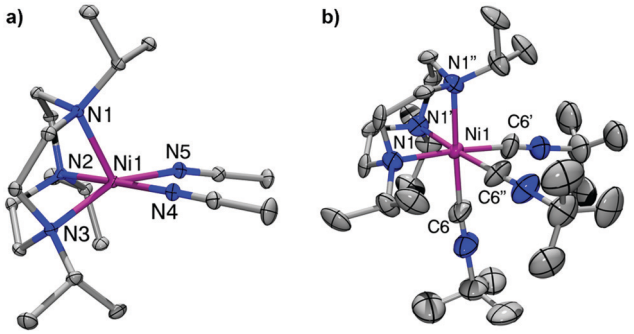

Fig. 3 ORTEP representation of the (a) solid-state structure of the cation of **3** with 50% probability ellipsoids. Selected bond lengths (Å): Ni1–N1 2.057(10); Ni1–N2 2.086(10); Ni1–N3 2.073(10); Ni1–N4 2.057(10); Ni1–N5 2.043(10); (b) Solid-state structure of the cation of **4** with 50% probability ellipsoids. Selected bond lengths (Å): Ni1–N1, 2.125(5); Ni1–C6, 1.946(8); C6–N2, 1.112(12) Hydrogen atoms, non-coordinated solvent molecules, and anions omitted for clarity.

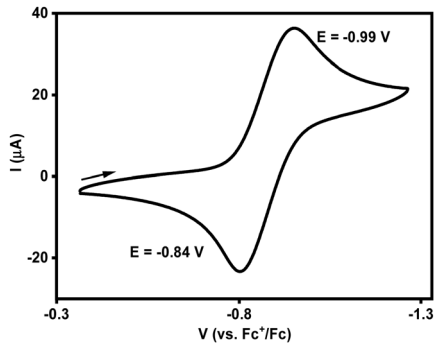

Fig. 4 CV of **4** in 0.1 M n-Bu_4NPF_6/MeCN (100 mV s^{-1} scan rate).

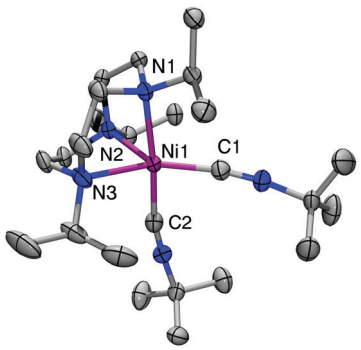

Fig. 5 ORTEP representation of the solid-state structure of the cation of **5** with 50% probability ellipsoids. Hydrogen atoms and anions omitted for clarity. Selected bond lengths (Å): Ni1–N1, 2.2044(19); Ni1–N2, 2.195(2); Ni1–N3, 2.198(2); Ni1–C1, 1.854(3) Ni1–C2, 1.933(3); C1–N4, 1.166(4); C2–N5, 1.151(3).

high-coordinate Ni(I) complexes and fewer containing redox innocent N-based ligands.[5] To the best of our knowledge, this 5-coordinate complex is the first isolated Ni(I) complex supported by a N-based, redox innocent, TACN ligand framework.

Furthermore, the characteristic C≡N bond stretches for the Ni-bound ^{t}BuNC species were observed by IR. For the Ni(I) complex **5** a main stretch of $\nu_{C\equiv N}$ = 2165 cm^{-1} was observed, within the range of reported Ni–CNR vibrational frequencies.[40–42] Importantly, for the Ni(II) complex **4**, the a higher main energy stretch of $\nu_{C\equiv N}$ = 2207 cm^{-1} was observed. These results are expected as the more electron rich Ni(I) is likely to π-backbond to the ^{t}BuNC to a greater extent, which leads to the shift of the $\nu_{C\equiv N}$ stretch to lower energy.[43]

EPR studies of **5** in a 1 : 3 MeCN:PrCN glass 77 K display a rhombic signal, consistent with a d^9 Ni(I) center (Fig. 6a). The simulated spectrum employed g values of g_x = 2.171, g_y = 2.121, and g_z = 2.018, a superhyperfine coupling constant of 11 G in the g_z direction to from one N (I = 1) atom from the iPr_3TACN ligand. Notably, the Density Functional Theory (DFT)-calculated g values of 2.044, 2.198, and 2.264 agree well with the experimental EPR values. In addition, the DFT-calculated spin density was also consistent with a Ni-based unpaired electron distributed between the d_{z^2} and $d_{x^2-y^2}$ atomic orbitals (Fig. 6b). Bulk analysis of **5** in solution *via* the Evans method reveals a magnetic moment μ_{eff} = 1.68 μ_B, confirming the presence of one unpaired electron. We suspect that the bulky iPr_3TACN ligand enforces a distortion in **5**, which leads to an elongation of the Ni–N bonds and a weaker interaction between the axial nitrogen atom and the Ni(I) center. In fact, a closer look at the metrical parameters of **5** reveals a slight bend of Ni(I)–C≡NR bond angles to an average value of 169.2°, likely due to the steric clash between ^{t}BuNC and the isopropyl N-substituents. A similar effect was observed by Hillhouse *et al.* for the Ni(I) metal center $[(IPr)Ni(CN^tBu)_3][B(Ar^F)_4]$ supported by a sterically encumbering N-heterocyclic carbene ligand and three distorted ^{t}BuNC ligands that exhibited an average Ni(I)–C≡NR bond angle of 171.2°.[44]

As a direct comparison to the iPr_3TACN-supported complexes described above, we decided to synthesize the analogous Me_3TACN derivatives. Using the same synthetic method as for **5** (Fig. 3), we have employed the $[(Me_3TACN)Ni(II)(MeCN)_3](BF_4)_2$ complex[38] as a suspension in THF and added 3 equiv. of ^{t}BuNC, to obtain the putative $[(Me_3TACN)Ni(II)(CN^tBu)_3](BF_4)_2$ as a pale green solid in 90% yield. The *in situ* reduction of $[(Me_3TACN)Ni(II)(CN^tBu)_3](BF_4)_2$ with 1 equiv. of cobaltocene in a 1 : 3

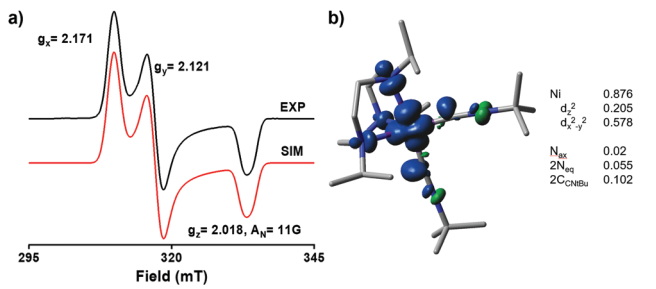

Fig. 6 (a) Experimental (1 : 3 MeCN:PrCN glass, 77 K) and simulated EPR spectra of **5**. The following parameters were used for simulation: g_x = 2.171; g_y = 2.121; g_z = 2.018 (A_N = 11.0 G). (b) DFT-calculated Mulliken spin density for **5** (shown at a 0.002 isodensity contour plot).

THF:2-MeTHF solvent and analysis by EPR at 77 K revealed a rhombic EPR spectrum, similar to the one observed for **5**. Slightly different g values of g_x = 2.165, g_y = 2.111, and g_z = 2.018 were observed, along with a slightly higher superhyperfine coupling constant of 12 G from the interaction with the axial N-atom (Fig. S15, ESI†). The slightly higher coupling constant is in line with a decrease in steric bulk of the N-Me substituents in Me_3TACN that allow for a tighter interaction with the Ni(I) center. Notably, the $[(Me_3TACN)Ni(I)(CN^tBu)_2]^+$ species was significantly less stable than **5** and could not be isolated due to its rapid decomposition within minutes at room temperature. On the other hand, complex **5** proved to be stable in solution, with no signs of decomposition after hours at RT. Overall, all these results highlight the key properties of the iPr_3TACN ligand, especially the importance of the appropriately bulky N-isopropyl groups and their ability to further stabilize the reactive metal species by sterically encumbering the low-valent Ni(I) center.

In summary, a $\{NiNO\}^{10}$ Ni-nitrosyl complex supported by the iPr_3TACN ligand was isolated in quantitative yield from *in situ* formation of a Ni(I) species and its further reaction with NO. These results suggested that iPr_3TACN should allow that stabilization of low-valent Ni species and led us to pursue the isolation of Ni(I) complexes supported by π-acceptor ligands. We have also reported the synthesis and characterization of a Ni(II) bis-solvento MeCN complex **3**, a potentially useful Ni precursor for catalytic applications. Furthermore, the presence of ^{t}BuNC as an ancillary ligand allowed for the isolation of a rare 5-coordinate $[(iPr_3TACN)Ni(I)(CN^tBu)_2](PF_6)$ complex **5**, which was characterized in detail *via* X-ray crystallography, EPR, IR, UV-Vis, and DFT calculations.

Conflicts of interest

There are no conflict to declare.

References

1 X. Hu, *Chem. Sci.*, 2011, **2**, 1867–1886.
2 J. Diccianni, Q. Lin and T. Diao, *Acc. Chem. Res.*, 2020, **53**, 906–919.
3 V. B. Phapale and D. J. Cardenas, *Chem. Soc. Rev.*, 2009, **38**, 1598–1607.
4 S. Z. Tasker, E. A. Standley and T. F. Jamison, *Nature*, 2014, **509**, 299–309.
5 C. Y. Lin and P. P. Power, *Chem. Soc. Rev.*, 2017, **46**, 5347–5399.
6 J. R. Zhou and G. C. Fu, *J. Am. Chem. Soc.*, 2003, **125**, 14726–14727.
7 O. Vechorkin and X. Hu, *Angew. Chem., Int. Ed.*, 2009, **48**, 2937–2940.
8 G. D. Jones, J. L. Martin, C. McFarland, O. R. Allen, R. E. Hall, A. D. Haley, R. J. Brandon, T. Konovalova, P. J. Desrochers, P. Pulay and D. A. Vicic, *J. Am. Chem. Soc.*, 2006, **128**, 13175–13183.
9 X. L. Yu, T. Yang, S. L. Wang, H. L. Xu and H. G. Gong, *Org. Lett.*, 2011, **13**, 2138–2141.
10 H. Yin and G. C. Fu, *J. Am. Chem. Soc.*, 2019, **141**, 15433–15440.
11 M. I. Lipschutz, X. Yang, R. Chatterjee and T. D. Tilley, *J. Am. Chem. Soc.*, 2013, **135**, 15298.
12 M. I. Lipschutz and T. D. Tilley, *Angew. Chem., Int. Ed.*, 2014, **53**, 7290–7294.
13 A. C. Manesis, B. W. Musselman, B. C. Keegan, J. Shearer, N. Lehnert and H. S. Shafaat, *Inorg. Chem.*, 2019, **58**, 8969–8982.
14 A. C. Manesis, M. J. O'Connor, C. R. Schneider and H. S. Shafaat, *J. Am. Chem. Soc.*, 2017, **139**, 10328–10338.
15 E. C. Kisgeropoulos, A. C. Manesis and H. S. Shafaat, *J. Am. Chem. Soc.*, 2021, **143**, 849–867.
16 S. I. Ting, W. L. Williams and A. G. Doyle, *J. Am. Chem. Soc.*, 2022, **144**, 5575–5582.
17 S. M. Smith, N. P. Rath and L. M. Mirica, *Organometallics*, 2019, **38**, 3602–3609.
18 M. B. Watson, N. P. Rath and L. M. Mirica, *J. Am. Chem. Soc.*, 2017, **139**, 35–38.
19 J. W. Schultz, K. Fuchigami, B. Zheng, N. P. Rath and L. M. Mirica, *J. Am. Chem. Soc.*, 2016, **138**, 12928–12934.
20 B. Zheng, F. Z. Tang, J. Luo, J. W. Schultz, N. P. Rath and L. M. Mirica, *J. Am. Chem. Soc.*, 2014, **136**, 6499–6504.
21 W. Zhou, S. A. Zheng, J. W. Schultz, N. P. Rath and L. M. Mirica, *J. Am. Chem. Soc.*, 2016, **138**, 5777–5780.
22 W. Zhou, M. B. Watson, S. Zheng, N. P. Rath and L. M. Mirica, *Dalton Trans.*, 2016, **137**, 15886–15893.
23 W. Zhou, N. P. Rath and L. M. Mirica, *Dalton Trans.*, 2016, **45**, 8693–8695.
24 W. Zhou, J. W. Schultz, N. P. Rath and L. M. Mirica, *J. Am. Chem. Soc.*, 2015, **137**, 7604–7607.
25 S. M. Smith, O. Planas, L. Gomez, N. Rath, X. Ribas and L. M. Mirica, *Chem. Sci.*, 2019, **10**, 10366–10372.
26 K. Fuchigami, M. B. Watson, G. N. Tran, N. P. Rath and L. M. Mirica, *Organometallics*, 2021, **40**, 2283–2289.
27 See ESI†.
28 B. C. Fullmer, M. Pink, H. J. Fan, X. F. Yang, M. H. Baik and K. G. Caulton, *Inorg. Chem.*, 2008, **47**, 3888–3892.
29 S. C. Puiu and T. H. Warren, *Organometallics*, 2003, **22**, 3974–3976.
30 A. M. Wright, G. Wu and T. W. Hayton, *J. Am. Chem. Soc.*, 2012, **134**, 9930–9933.
31 A. M. Wright and T. W. Hayton, *Comments Inorg. Chem.*, 2012, **33**, 207–248.
32 J. H. Enemark and R. D. Feltham, *Coord. Chem. Rev.*, 1974, **13**, 339–406.
33 V. K. Landry, K. L. Pang, S. M. Quan and G. Parkin, *Dalton Trans.*, 2007, 820–824.
34 S. Soma, C. Van Stappen, M. Kiss, R. K. Szilagyi, N. Lehnert and K. Fujisawa, *J. Biol. Inorg. Chem.*, 2016, **21**, 757–775.
35 D. Steinborn, *J. Chem. Educ.*, 2004, **81**, 1148–1154.
36 J. N. Rebilly, G. Charron, E. Riviere, R. Guillot, A. L. Barra, M. D. Serrano, J. van Slageren and T. Mallah, *Chem. – Eur. J.*, 2008, **14**, 1169–1177.
37 J.-N. Rebilly, L. Catala, E. Rivière, R. Guillot, W. Wernsdorfer and T. Mallah, *Inorg. Chem.*, 2005, **44**, 8194–8196.
38 H. Tak, H. Lee, J. Kang and J. Cho, *Inorg. Chem. Front.*, 2016, **3**, 157–163.
39 C. R. Groom, I. J. Bruno, M. P. Lightfoot and S. C. Ward, *Acta Crystallogr., Sect. B: Struct. Sci., Cryst. Eng. Mater.*, 2016, **72**, 171–179.
40 A. K. Maity, M. Zeller and C. Uyeda, *Organometallics*, 2018, **37**, 2437–2441.
41 C. A. Laskowski, D. J. Bungum, S. M. Baldwin, S. A. Del Ciello, V. M. Iluc and G. L. Hillhouse, *J. Am. Chem. Soc.*, 2013, **135**, 18272–18275.
42 B. J. Fox, M. D. Millard, A. G. DiPasquale, A. L. Rheingold and J. S. Figueroa, *Angew. Chem., Int. Ed.*, 2009, **48**, 3473–3477.
43 P. M. Treichel, in *Adv. Organomet. Chem.*, ed. F. G. A. Stone and R. West, Academic Press, 1973, vol. 11, pp. 21–86.
44 C. A. Laskowski and G. L. Hillhouse, *Chem. Sci.*, 2011, **2**, 321–325.